Synthesis and Characterization of Au@Co and Au@Ni Core−Shell Nanoparticles and Their Applications in Surface-Enhanced Raman Spectroscopy

ARTICLE *in* THE JOURNAL OF PHYSICAL CHEMISTRY C · DECEMBER 2007

Impact Factor: 4.77 · DOI: 10.1021/jp075844k

5 AUTHORS, INCLUDING:

Bin Ren
Xiamen University
272 PUBLICATIONS **8,594** CITATIONS
SEE PROFILE

Zhong-Qun Tian
Xiamen University
355 PUBLICATIONS **10,098** CITATIONS
SEE PROFILE

Synthesis and Characterization of Au@Co and Au@Ni Core−Shell Nanoparticles and Their Applications in Surface-Enhanced Raman Spectroscopy

Fang Bao,[†] Jian-Feng Li,[‡] Bin Ren,*[,‡] Jian-LinYao,[†] Ren-Ao Gu,*[,†] and Zhong-Qun Tian[‡]

Department of Chemistry, Suzhou University, Suzhou 215006, China, and State Key Laboratory for Physical Chemistry of Solid Surfaces and Department of Chemistry, College of Chemistry and Chemical Engineering, Xiamen University, Xiamen 361005, China

Received: July 25, 2007; In Final Form: September 21, 2007

Au@Co and Au@Ni core−shell nanoparticles with controllable shell thicknesses were prepared by reduction of Co^{2+} and Ni^{2+} salts with hydrazine hydrate in ethanol over preformed Au seeds. Both cyclic voltammetric and surface-enhanced Raman studies using CO as the probe molecule confirmed the core−shell structure of the synthesized nanoparticles. The Au@Co and Au@Ni nanoparticles dispersed on a glassy carbon electrode surface exhibit high surface-enhanced Raman scattering (SERS) effect for the adsorbed pyridine. High-quality SERS spectra of CO absorbed on Co and Ni have been obtained through the high enhancement of the core−shell nanoparticles. The originally low surface enhancement of the Co and Ni can be substantially improved giving total enhancement factors up to 10^3−10^4. Such a SERS-active substrate can be used as an alternative substrate for investigating adsorption and reactions occurring on the Co and Ni metal surfaces.

Introduction

Metal nanoparticles may exhibit very unique electrical, optical, magnetic, and chemical properties that are not achievable by their bulk counterparts.[1,2] Transition-metal materials, especially Fe, Co, and Ni, have been extensively studied, as a result of their important applications in fields such as catalysis, solar energy absorption, permanent magnets, magnetic fluids, and magnetic recording media.[3,4] Many methods have been used in the preparation of Co and Ni nanoparticles, such as metal carbonyl pyrolysis, electrochemical deposition, and solution-phase metal salt reduction.[5−8] The redox procedure using hydrazine hydrate as the reducing agent is facile and inexpensive, and the product does not display chemical contamination from reducing agents.[9−12]

Surface-enhanced Raman spectroscopy (SERS) is an important tool to characterize the process occurring on metal surfaces on the molecular level.[13−15] Especially from the mid-1990s, Tian's group has made various approaches to optimize the detection sensitivity of a confocal Raman microscope and, further, to develop surface roughening procedures for different transition metals, such as Pt, Rh, Pd, Fe, Co, and Ni, through which good-quality surface Raman signals have been obtained.[16] As a consequence, it has become feasible to carry out SERS investigations on diverse molecules on many transition-metal substrates.[17] However, it must be emphasized that the SERS activity of pure transition metals is still rather weak; the SERS signal of some adsorbates with a very small Raman cross section or with a low surface coverage is still below the detection limit in comparison with coinage metals. Therefore, it is desirable to increase the SERS activity of transition-metal surfaces in order to improve molecular generality of SERS.

Another parallel development to pure transition metals is to coat ultrathin film of transition metals over the SERS-active noble metal core, whose high enhancement can affect to a certain distance away from the core via the long-range effect of the electromagnetic (EM) field.[18−21] Recently, a simpler and more straightforward method has been developed by the Tian group on the basis of a seed-mediated growth method,[22−24] in which Au nanoparticles serve as the seed in a solution where a second metal ion is chemically reduced on the surface of the seeds to form a shell layer, resulting in core−shell nanoparticles. Similar to the ultrathin film strategy, the long-range effect of the enhanced EM field generated by the highly SERS-active Au core can boost the surface enhancement on the surface of the ultrathin transition-metal shells (ca. 2−10 atomic layers).[25−26] Thereby, the original low surface enhancement of the transition metal can be substantially improved.[24] They have been able to obtain SERS signals from Au@Pt and Au@Pd nanoparticles surfaces.[27−30]

Bearing in mind the advantages of the above-mentioned approaches, it is desirable to extend the study to iron group metals, such as Ni and Co, to further develop this method into a general approach for SERS.

In the present work, we synthesize a series of Au@Co and Au@Ni nanoparticles using hydrazine hydrate as the reducing agent in ethanol. Au nanoparticles serve as seeds, over which Co or Ni ions are chemically reduced into a shell layer, resulting in core−shell nanoparticles. The size of the core−shell nanoparticles can be controlled by adjusting the amount of the Co or Ni ions to the Au seed. The size and electrochemistry properties of these nanoparticles were characterized by scanning electron microscopy (SEM) and cyclic voltammetry (CV). Carbon monoxide (CO) is used as a probe molecule to verify that the ultrathin shell is sufficient to completely cover the Au core. The SERS activities of these nanoparticles have been tested by using pyridine (Py) as a probe molecule. The total enhancement of as high as about three to four orders of magnitudes has been achieved, which makes it possible to carry out detailed

* To whom correspondence should be addressed. R. A. Gu: Phone, +86-512-65880399; Fax, +86-512-65880089; E-mail: ragu@suda.edu.cn. B. Ren: Phone, +86-592-2181906; E-mail: bren@xmu.edu.cn.

[†] Suzhou University.

[‡] Xiamen University.

10.1021/jp075844k CCC: $40.75
Published on Web 12/15/2007

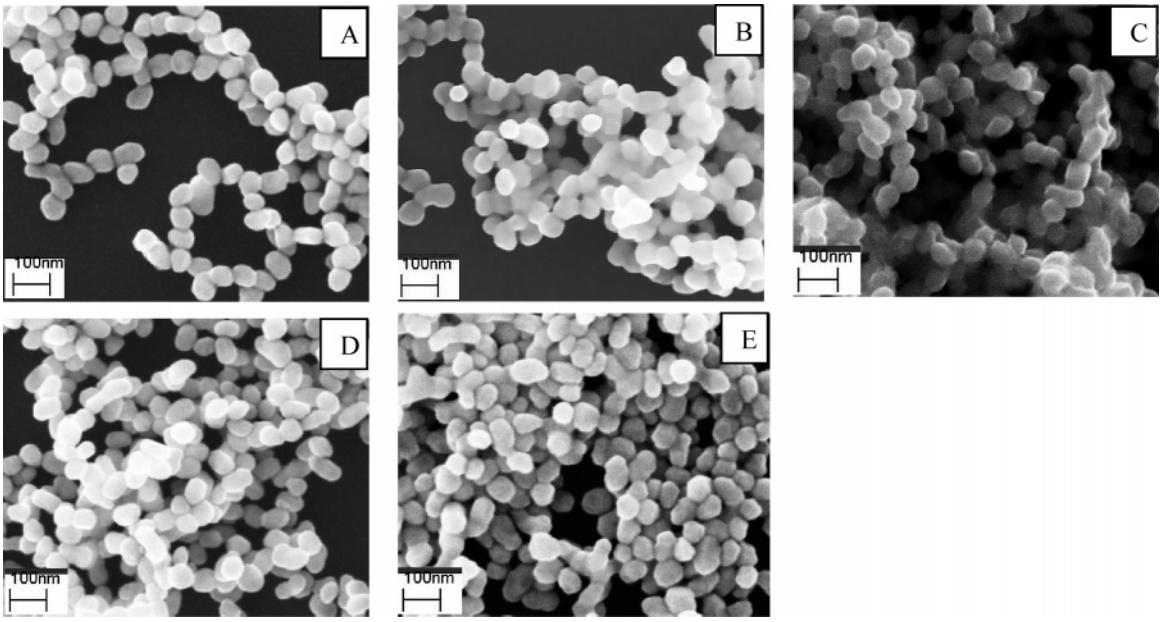

Figure 1. SEM images of Au seed (A); Au@Co nanoparticles synthesized with different volumes of $CoCl_2$: (B) 1.8 mL, (C) 5 mL; Au@Ni nanoparticles synthesized with different volumes of $NiCl_2$: (D) 1.8 mL, (E) 5 mL.

molecular-level investigation on some important molecules with small Raman cross section like CO.

2. Experiment Section

All chemicals were of analytical grade and were used as received. Aqueous solutions were prepared with Milli-Q water.

Synthesis of Au@Co and Au@Ni Core−Shell Nanoparticles. Au@Co and Au@Ni nanoparticles were synthesized by deposition of Co or Ni on the preformed Au nanoparticle seeds. The Au seeds were prepared according to Frens' method.[31] In brief, 200 mL of a 1% $HAuCl_4 \cdot 4H_2O$ aqueous solution was heated to boiling with vigorous stirring to which 1.3 mL of a 1% trisodium citrate solution was added. The mixture was then kept boiling for 30 min. Afterward, the solution was allowed to cool down to room temperature with continuous stirring. Then, 40 mL of Au colloid was taken out and centrifuged at 4000 rpm for 15 min. After the supernatant was removed, and solutions containing different amounts of 1 mmol/L $CoCl_2$ or $NiCl_2$ dissolved in ethanol (0.6, 1.8, 2.4, 3, and 5 mL) were added, which were ultrasonically dispersed. The $CoCl_2$ solution containing Au nanoparticles was dropped into a solution containing 0.1 mL of 50% hydrazine hydrate and 1 mL of 0.5 mol/L sodium hydroxide while stirring at 50 °C. After addition, the stirring was continued for 15 min. In the case of $NiCl_2$, the reaction had to take place at 65 °C, and the volume of hydrazine hydrate added to the $NiCl_2$ solution should be 0.3 mL.The resulting black sols were collected by centrifugation and washed with absolute ethanol and Milli-Q water in sequence for several times. A drop of the concentrated sols were then dispersed on a glassy carbon (GC) disk electrode ($d = 5$ mm) and dried in a desiccator. To ensure the reproducibility, the GC electrode should be first mechanically polished successively with fine emery paper and alumina powder down to 0.05 μm to obtain a mirror finish surface, followed by sonication in Milli-Q water for 3 min. A similar method was utilized to prepare GC supported Co-coated Au nanoparticle electrodes (Au@Co/GC electrodes), pure Au nanoparticles (Au/GC electrodes), and pure Co nanoparticles (Co/GC electrodes). A Pt ring and a saturated calomel electrode (SCE) served as the counter and reference electrodes, respectively. All the potentials were quoted vs SCE.

In the following sections, unless otherwise stated, the Au@Co and Au@Ni nanoparticles made by using 1.8 mL of $CoCl_2$ or $NiCl_2$ are used to demonstrate the electrochemical and SERS characteristics of the particles assembled on GC electrodes.

Characterization. In situ SERS measurements were carried out on a Labram I confocal microprobe Raman system (JY, France). The excitation wavelength is 632.8 nm from a He−Ne laser. The microscope objective for laser illumination and signal collection was of long working distance (8 mm) with 50× magnification and a numerical aperture of 0.55. All electrochemical measurements were performed in a conventional three-compartment glass cell by using an electrochemical workstation (CHI 631A, CH Instruments). SEM images were taken with a field mission microscope (Leo1530) operated at an accelerating voltage of 20 kV.

3. Results and Discussion

The size and morphology of the as-prepared products were examined by SEM. Parts A−D of Figure 1 are the SEM images of the Au seed and core−shell Au@Co and Au@Ni nanoparticles. Figure 1A gives an SEM image of the Au seeds with a mean diameter of ∼60 nm. After the Au seeds were coated by Co or Ni, both the Au@Co and Au@Ni nanoparticles show nearly spherical shape and fair uniformity. Most of the nanoparticles are agglomerated, which is probably due to the fact that Ni and Co are magnetic materials so they are quite unstable with respect to both coagulation and reactivity. No small particles were observed in these SEM images, indicating that the reduction of Co or Ni only took place on the surface of the Au seed. As shown in parts B−E of Figure 1, with the increase in the volume of the $CoCl_2$ or $NiCl_2$, the average size of the nanoparticles slightly increases. When 1.8 mL or 5 mL of the metal ions was added, the average size of the nanoparticles was about 63 ± 2 and 65 ± 2 nm, respectively. This final diameter of the core−shell nanoparticles corresponds to the size that is calculated according to the relation in the literature.[29] As the size of the nanoparticles is not narrowly distributed, it is difficult to find an obvious change in the particles after coated with shells. However, it is still possible to find from the following

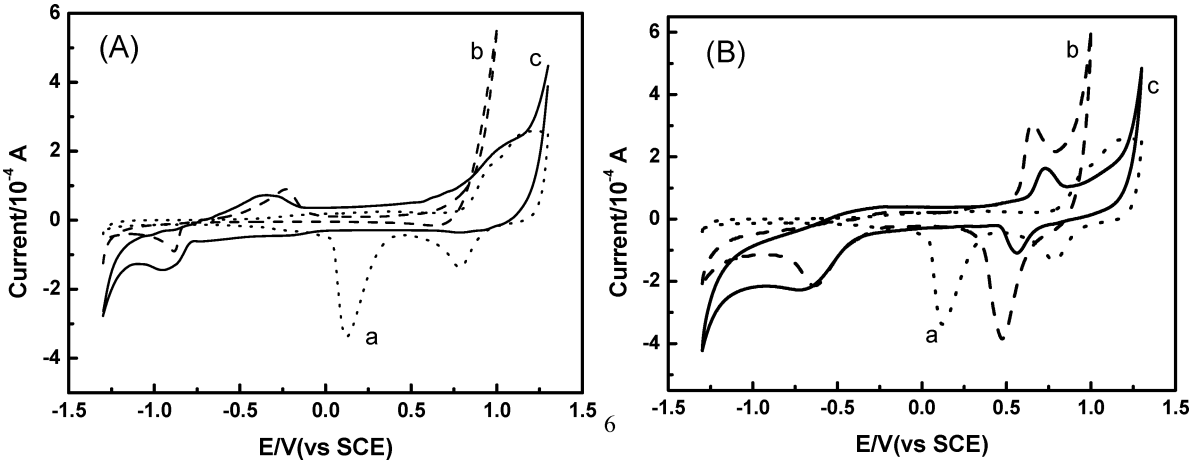

Figure 2. CV curves of different nanoparticles assembled on a GC electrode surface in 0.1 mol/L $NaClO_4$ solution. (A) (a) 60 nm Au; (b) Co nanoparticles; (c) ~62 nm Au@Co; (B) (a) 60 nm Au; (b) Ni nanoparticles; (c) ~62 nm Au@Ni. Au@Co and Au@Ni nanoparticles were prepared using 1.8 mL of $CoCl_2$ or $NiCl_2$. Scan rate = 50 mV/s.

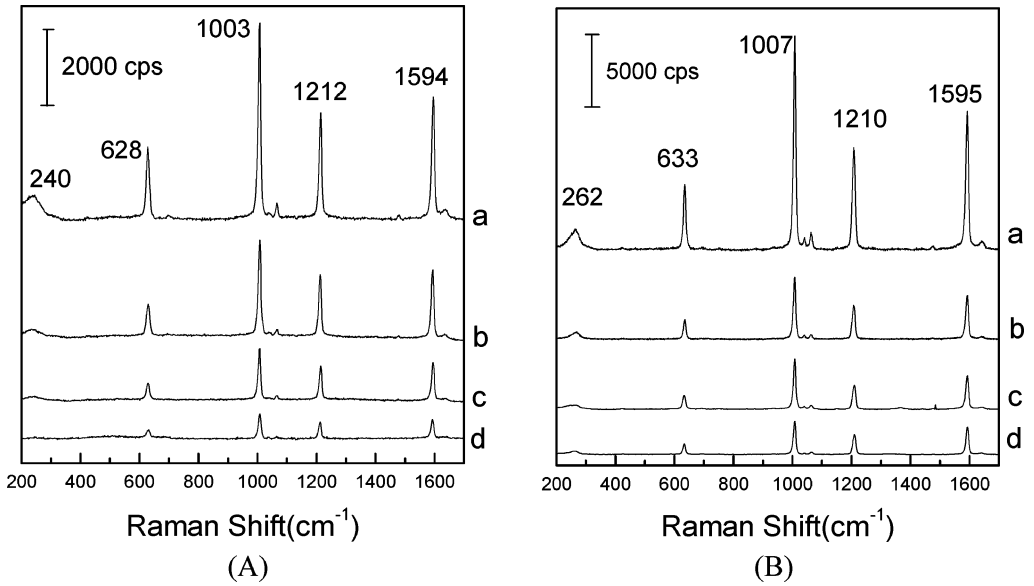

Figure 3. SERS spectra of Py on 60 nm Au@Co/GC with different Co thicknesses (A) and 60 nm Au@Ni/GC with different Ni thicknesses (B): (a) 0.6 nm, (b) 0.9 nm, (c) 1.5 nm, and (d) 2.5 nm of the Co or Ni shell at −1.0 V in 0.01 mol/L Py + 0.1 mol/L $NaClO_4$.

CV and SERS studies that the electrochemical and spectral properties of nanoparticles of different shell thickness are indeed different.

In order to examine the coating quality of the nanoparticles, we used CV, a surface sensitive technique, to check whether there are pinholes on the shell. CV curves of Au@Co/GC, Co/GC and Au@Ni/GC, Ni/GC electrodes and 60-nm Au-nanoparticles-modified GC electrode in 0.1 mol/L $NaClO_4$ are shown in parts A and B of Figure 2. The Co and Ni nanoparticles were prepared following the reported methods.[9,11] Figure 2A shows that, when Au nanoparticles are assembled on the GC surface, the CV curve shows typical surface reduction peaks at 0.12 and 0.78 V, which is similar to those of a bulk gold electrode.[32] The CV curve of the Au@Co/GC electrode shows an oxidation peak at about −0.35 V and a reduction peak at about −0.92 V, similar to that of the Co/GC electrode, indicating that the Au@Co/GC electrode is representative of the electrochemical properties of the pure Co surface. The result indicates that the particles have a $Au_{core}-Co_{shell}$ structure, even after being assembled on a surface. The absence of Au reduction peaks indicates that the Au core is completely covered by the Co shell and that there is no discernible Au site. However, the oxidation peak of Au@Co/GC is still slightly different from that of Co/GC, indicating that the ultrathin shell is slightly different from that of the bulk Co surface. Accordingly, we consider that a shell thickness of 5 nm is the optimal condition in using Au@Co and Au@Ni nanoparticles for electrochemical investigation. Similar to the Au@Co/GC case, the CV curve of Au@Ni/GC resembles that of the Ni/GC electrode, with the oxidation peak and the reduction peaks at about 0.72 and 0.55 and −0.69 V, respectively. The absence of Au reduction peaks also supports that the Au core is completely covered by the ultrathin Ni shell.

To test the SERS activity of the as-prepared Au@Co and Au@Ni nanoparticles, Py, a widely used Raman probe molecule because of its large Raman cross section, was selected as the probe molecule. Figure 3 is the SERS spectra of Py on the Au@Co/GC electrode (A) and Au@Ni/GC electrode (B) with different shell thicknesses, respectively. The spectra were obtained at −1.0 V in 0.01 mol/L Py + 0.1 mol/L $NaClO_4$. Four most enhanced bands appeared near 633, 1007, 1212, and 1593 cm^{-1}. They are attributed to the ring in-plane deformation (ν_{6a}), ring breathing (ν_1), C−H in-plane deformation (ν_{9a}), and ring stretching (ν_{8a}) vibrations, respectively. In addition, a broad and weak band at ca. 258 cm^{-1}, assigned to Co−N and Ni−N, was also observed.[33,34] As can be seen in Figure 5, the thinner the Co or Ni shell, the stronger the SERS signal that can be

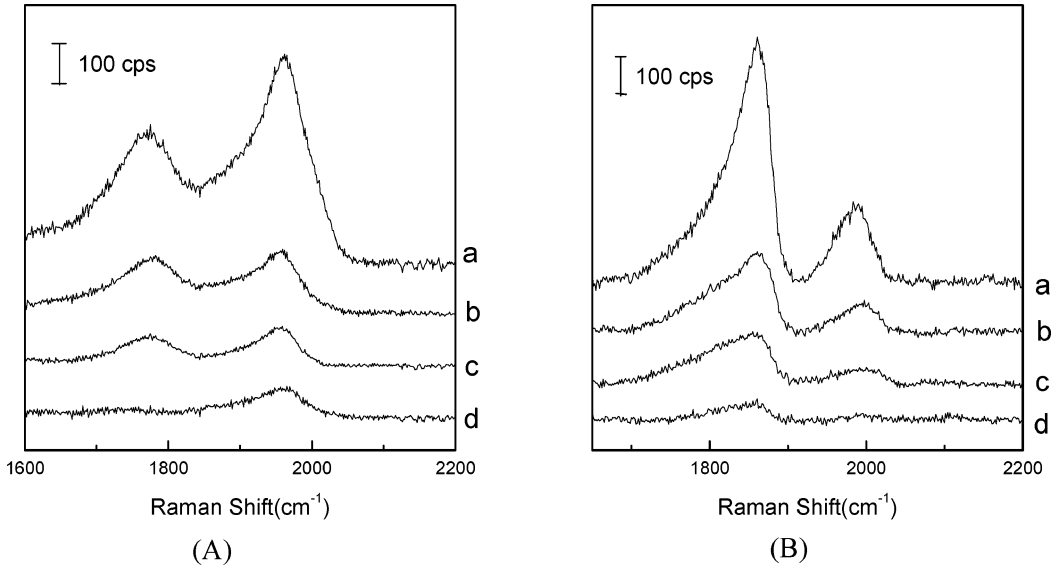

Figure 4. SERS spectra of CO adsorbed on 60 nm Au@Co/GC with different Co thicknesses (A) and 60 nm Au@Ni/GC with different Ni thicknesses (B): (a) 0.3 nm, (b) 0.9 nm, (c) 1.2 nm, and (d) 1.5 nm of the Co or Ni shell at −1.0 V in 0.1 mol/L $NaClO_4$.

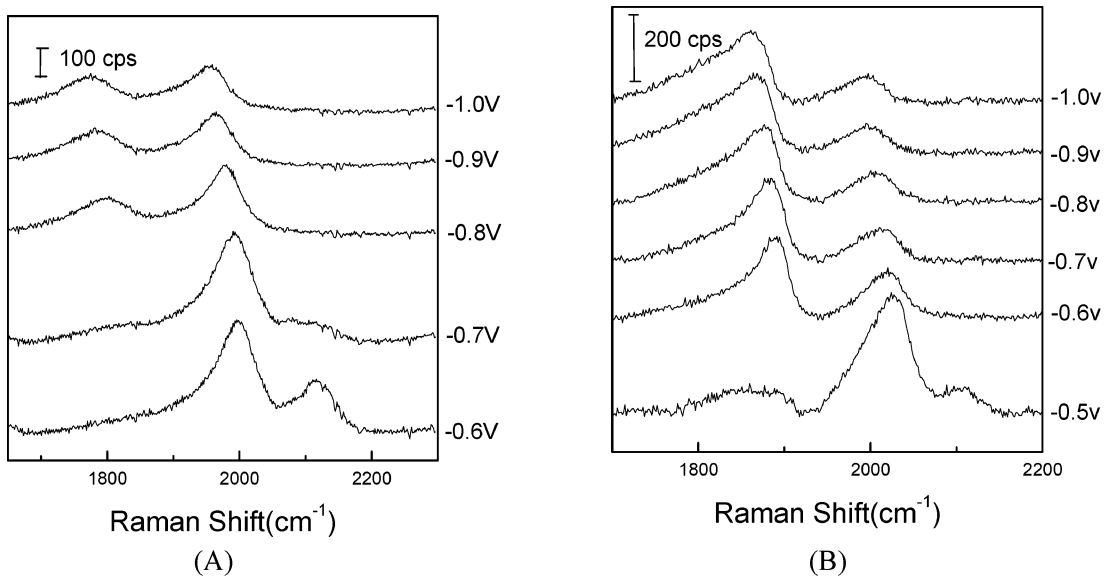

Figure 5. Potential-dependent SERS spectra of Au@Co/GC (A) and Au@Ni/GC (B) in 0.1 mol/L $NaClO_4$ after being held at −1.0 V in 0.1 mol/L $NaClO_4$ saturated with CO.

obtained from the substrate. Because of the unrealistic calculation demand on considering the thickness of 0.3 nm, the thinnest shell thickness is set to 0.6 nm. The SERS signal of the strongest band of Py from the 60nmAu@1.5nmCo/GC and 60nmAu@1.5nmNi/GC is about 20- and 50-fold stronger than that of roughened massive Co[33] and Ni[34] electrodes, respectively. By consideration that the roughness factor of the roughened electrode is about 4.2 for Co and Ni and that of core−shell nanoparticles film electrodes is about 15, one would expect the surface enhancement factor for the core−shell nanoparticles was evaluated at the level of 10^3-10^4, it is to be about 6-fold larger than that for the roughened electrode of Co[33] and 14-fold for Ni.[34]

One may still doubt whether the so strong SERS activity is really from the transition-metal shell. May it come from the exposed Au core due to the existence of some pinholes on the surface of the core−shell nanoparticles? To verify that the ultrathin shell is sufficient to completely cover the Au core at the molecular level, we used CO as a probe molecule. As CO band position is very sensitive to the nature of the metal, they can be used to identify the property of the substrate. The SERS spectra of CO adsorbed on Au@Co/GC with different Co shell thickness and Au@Ni/GC with different Ni shell thickness are shown in parts A and B of Figure 4. All the spectra were acquired at −1.0 V in 0.1 mol/L $NaClO_4$ solution saturated with CO. In Figure 4A, the band at about 1780 and 1960 cm^{-1} can be assigned to bridge- and linear-bonded CO, respectively.[35] The band at ca. 2110−2135 cm^{-1} corresponding to the stretching of CO bound to Au[36] is absent even when the thickness of the Co shell is as thin as 0.3 nm, which clearly demonstrates the pinhole-free nature of the Co shells, i.e., the thin Co shell is sufficient to screen the chemical properties of Au. It can also be seen from the figure that the SERS intensity of CO decreases significantly with the increasing shell thickness, which follows essentially the same trends as that using Py as the probe molecule. This phenomenon indicates that the high SERS activity obtained from the ultrathin Co shell is attributed to the long-range effect of the EM field of the Au core. The appearance of both bridge- and linear-bonded CO is in good agreement with the previous EELS study of a polycrystalline

Co system.[35] Similar to the Au@Co/GC system, both bridge- and linear-bonded CO were observed at about 1860 and 1994 cm^{-1} on Au@Ni/GC (Figure 4B), respectively, and the signal related to CO bound to Au is also absent. However, we did not observe obvious differences in the CO band frequency no matter whether the thickness is 0.3 or 1.5 nm for both Co and Ni, although CO is well-known to be extremely sensitive to the electronic properties of the substrate. This phenomenon is still hard to understand at present and requires more systematic study both experimentally and theoretically.

It should be especially pointed out that, the SERS spectra of CO absorbed on Co and Ni shown above are of very high quality, which is impractical and difficult to obtain by using the enhancement of SERS of transition metals themselves. In fact, to our best knowledge, this is the first report on the SERS of CO adsorbed on Co and Ni. Such a high enhancement allows us to further explore the detailed electrochemical behavior of CO absorbed on these core−shell nanoparticles. For this purpose, we studied the potential-dependent behavior of CO adsorbed on Au@Co/GC (Figure 5A) and Au@Ni/GC (Figure 5B) using SERS. Similar to Figure 4B, mainly two ν_{CO} bands are found on the Au@Ni/GC surface; the bands at 1940−2050 cm^{-1} can be assigned to linear-bonded CO (CO_L), and those at 1800−1930 cm^{-1} correspond to bridge-bonded CO (CO_B). The spectra shown were acquired at −1.0 V in 0.1 mol/L $NaClO_4$ solution saturated with CO, starting from the largest negative potential to more positive potential. In the potential region between −1.0 and −0.6 V, the frequency of these bands increases with the positive movement of the electrode potential, and the intensity remains constant until at −0.6 V where the frequency and the intensity of CO_B band begin to decrease, but the intensity of CO_L band starts to increase. The appearance of both bands for Au@Ni/GC in a neutral electrolyte is in agreement with previous SEIRAS measurement,[37] and a similar trend of intensity change with potential also had been found. It can also be seen that the CO_B bands are more intense than the CO_L bands, indicating that CO absorbed on polycrystalline Ni surface mainly with the bridge site in the potential range investigated. When the potential is further positively moved to −0.5 V, the oxidation potential of the Ni shell, some sites of the underlayer Au start to be exposed, evidenced by a small band at 2110 cm^{-1} attributed to the adsorbed CO on Au.[36] Thus, the intensity of the CO_L band become more intense at this potential as somewhat Ni on the surface has been dissolved and then the Ni shell become thinner.

A series of potential-dependent SERS spectra of CO adsorbed on Au@Co/GC is shown in Figure 5A, and the SERS spectra were obtained in the same fashion as Au@Ni/GC. In comparison with the Au@Ni/GC case, a similar phenomenon was observed on Au@Co/GC, in addition several unique features have also been observed. Two major ν_{CO} bands were observed, a band at 1700−1870 cm^{-1} and a stronger band at 1880−2060 cm^{-1}. According to the previous EELS obtained for the polycrystalline Co,[35] the high- and low-frequency ν_{CO} bands can be assigned to the linear- and bridge-bound CO, respectively. It is indicated that CO is adsorbed on the polycrystalline Co surface mostly on the linear on-top site, which is different from the Au@Ni/GC case. Furthermore, the frequency of both bands increases with increasing potential until −0.6 V, where some Au sites are exposed at a negative potential after the oxidation of the Co surface. This phenomenon is similar to that in the Au@Ni/GC case. The different spectral behaviors are presumably determined by the chemical activity and properties of the different transition metals.

The above preliminary studies of CO adsorbed on Co and Ni clearly show that with its high surface enhancement ultrathin-layer core−shell nanoparticles can be effectively used to study systems with extremely low Raman cross sections, which may pave the way for expanding the molecular systems that can be investigated using Raman spectroscopy.

4. Conclusion

Core−shell Au@Co and Au@Ni nanoparticles with different shell thicknesses have been prepared by the Au seed-mediated chemical reduction method. The core−shell nanoparticles exhibited the similar electrochemical properties to the Co or Ni nanoparticles surface. These nanoparticles show very high SERS activities, with the maximal enhancement in the range of 200 to 1700 cm^{-1} using Py as a probe molecule. With the increase of the shell thickness, the SERS intensity decreases significantly, indicating that the high SERS activity obtained from the ultrathin shell system is attributed to the long-range effect of the EM field of the Au core. The ultrathin shell was found to be sufficient to completely cover the Au core, using a substrate sensitive molecule, CO. The result convincingly shows that the core−shell nanoparticles are pinhole free. High-quality potential-dependent SERS spectra of CO on Co and Ni have been obtained via the high enhancement of this kind of nanoparticles. The ability to detect in situ the vibrational properties of adsorbates with very small Raman cross sections reveals that the core−shell strategy can be used to study the catalytic reactions occurring on Co and Ni surfaces.

Acknowledgment. This work was supported by the Natural Science Foundation of China and the financial support of State Key Laboratory for Physical Chemistry of Solid Surfaces of Xiamen University. The Raman spectroscopy experiments were carried out in Xiamen University. The authors are grateful for the kind help of the co-workers there. We gratefully acknowledge the support from the Natural Science Foundation of China (NSFC) (20573076, 20503019), the NSF of Jiangsu Province-(BK2005032), and the Specialized Research Fund for the Doctoral Program of Higher Education (SRFDP) (20050285019).

References and Notes

(1) Majetich, S. A.; Jin, Y. *Science* **1999**, *284*, 470.
(2) Zarur, A. J.; Ying, J. Y. *Nature* **2000**, *403*, 65.
(3) Teng, U. J.; X. W.; Wang, Y.; Yang, H.; Xia, Y. N. *Adv. Mater.* **2007**, *19*, 33.
(4) Bergemann, C.; Muller-Schulte, D.; Oster, J.; Brassard, L.; Lubbe, A. S. *J. Magn. Magn. Mater.* **1999**, *194*, 45.
(5) Cheng, G. J.; Romero, D.; Gerald, T, F.; Hight, Walker, A. R. *Langmuir* **2005**, *21*, 12055.
(6) Whitney, T. M.; Jiang, J. S.; Searson, P. C.; Chien, C. L. *Science* **1993**, *261*, 316.
(7) Sun, S.; Murray, C. B. *J. Appl. Phys.* **1999**, *85*, 4325.
(8) Sun, Y. P.; Rollins, H. W.; Guduru, R. *Chem. Mater.* **1999**, *11*, 7.
(9) Zhu, Y. C.; Zheng, H. H.; Yang, Q.; Pan, A. L.; Yang, Z. P.; Qian, Y. T. *J. Cryst. Growth* **2004**, *260*, 427.
(10) Guo, F.; Zheng, H. G.; Yang, Z. P.; Qian, Y. T. *Mater. Lett.* **2002**, *56*, 906.
(11) Wu, S. H.; Chen, D. H. *J. Colloid Interface Sci.* **2003**, *259*, 282.
(12) Li, Z. Y.; Han, C. G. *J. Mater. Sci.* **2006**, *41*, 3473.
(13) Kneipp, K.; Kneipp, H.; Itzkan, I.; Dasari, R. R.; Feld, M. S. *J. Phys.: Condens. Matter.* **2002**, *14*, R597.
(14) Cao, Y. C.; Jin, R.; Mirkin, C. A. *Science* **2002**, *297*, 1536.
(15) Mrozek, M. F.; Weaver, M. J. *Anal. Chem.* **2002**, *74*, 4069.
(16) Tian, Z. Q.; Ren, B.; Wu, D. Y. *J. Phys. Chem. B* **2002**, *106*, 9463.
(17) Tian, Z. Q.; Ren, B. *Annu. Rev. Phys. Chem.* **2004**, *55*, 197.
(18) Leung, L. W. H.; Weaver, M. J. *J. Electroanal. Chem.* **1987**, *217*, 367.
(19) Leung, L. W. H.; Weaver, M. J. *J. Am. Chem. Soc.* **1987**, *109*, 5113.
(20) Leung, L. W. H.; Weaver, M. J. *Langmuir* **1988**, *4*, 1076.

(21) Fleischmann, M.; Tian, Z. Q. *J. Electroanal. Chem.* **1987**, *217*, 411.

(22) Tian, Z. Q.; Yang, Z. L.; Ren, B.; Li, J. F.; Zhang, Y.; Lin, X. F.; Hu, J. W.; Wu, D. Y. *Faraday Discuss.* **2006**, *132*, 159.

(23) Hu, J. W.; Zhang, Y.; Li, J. F.; Liu, Z.; Ren, B.; Sun, S. G.; Tian, Z. Q.; Lian, T. *Chem. Phys. Lett.* **2005**, *408*, 354.

(24) Tian, Z. Q.; Ren, B.; Li, J. F.;Yang, Z. L. *Chem. Commun.* **2007**, *1*.

(25) Aravind, P. K.; Nitzan, A.; Metiu, H. *Surf. Sci.* **1981**, *110*, 189.

(26) Nitzan, A.; Brus, L. E. *J. Chem. Phys.* **1981**, *75*, 2205.

(27) Lu, L. H.; Wang, H. S.; Xi, S. Q.; Zhang, H. J. *J. Mater. Chem.* **2002**, *12*, 156.

(28) Lu, L. H.; Sun, G. Y.; Zhang, H. J.; Wang, H. S.; Xi, S. Q.; Hu, J. Q.; Tian, Z. Q.; Chen, R. *J. Mater. Chem.* **2004**, *14*, 1005.

(29) Zhang, B.; Li, J. F.; Zhong, Q. L.; Ren, B.; Tian, Z. Q.; Zou, S. Z. *Langmuir* **2005**, *21*, 16.

(30) Li, J. F.; Yang, Z. L.; Ren, B.; Liu, G. K.; Fang, P. P.; Jiang, Y. X.; Wu, D. Y.; Tian, Z. Q. *Langmuir* **2006**, *22*, 10372.

(31) Frens, G. *Nat. Phys. Sci.* **1973**, *241*, 20.

(32) Richard, P, J.; W Ronald, F. *J. Phys. Chem. B* **1997**, *101*, 8550.

(33) Wu, D. Y.; Xie, Y.; Ren, B.; Yan, J. W.; Mao, B. W.; Tian, Z. Q. *Phys. Chem. Commun.* **2001**, *18*, 1.

(34) Huang, Q. J.; Lin, X. F.; Yang, Z. L.; Hu, J. W.; Tian, Z. Q. *J. Electroanal. Chem.* **2004**, *563*, 121.

(35) Rao, C. N. R; Kamath, V.; Prabhakaran, K.; Hegde, M. S. *Can. J. Chem.* **1985**, *63*, 1780.

(36) Andrzej, K.; Bruno, P. *Chem. Phys. Lett.* **2004**, *383*, 76.

(37) Huo, S. J.; Xue, X. K.; Yan, Y. G.; Li, Q. X.; Ma, M.; Cai, W. B.; Xu, Q. J.; Osawa, M. *J. Phys. Chem. B* **2006**, *110*, 4162.